

Clustering in a Compressible Particle Ladden Jet

Jörn Sesterhenn

Institute for Fluid Dynamics and Technical Acoustics

TECHNISCHE UNIVERSITÄT BERLIN

Aarhus Nov 6/7 2014



Volcanic Jet at Stromboli, May 2013



Numerical Modelling



Numerical Modelling

Compressible Navier-Stokes equations

Direct equations

conservation of mass

conservation of momentum

conservation of energy

Numerical Modelling

Compressible Navier-Stokes equations

Direct equations

$$\frac{\partial \rho}{\partial t} + \frac{\partial (\rho u_i)}{\partial x_i} = 0$$

$$\frac{\partial u_i}{\partial t} + u_j \frac{\partial u_i}{\partial x_j} = -\frac{1}{\varrho} \frac{\partial p}{\partial x_i} + \frac{1}{\varrho} \frac{\partial \tau_{ij}}{\partial x_j}$$

$$\frac{\partial s}{\partial t} + u_j \frac{\partial s}{\partial x_j} = -\frac{1}{\varrho T} \left(\frac{\partial}{\partial x_j} \left(\lambda \frac{\partial T}{\partial x_j} \right) + \Phi \right)$$

Point Particles Model

Compressible Navier-Stokes
Equation



Particle Equations

Point Particles Model

$$\frac{\partial \rho_f}{\partial t} + \frac{\partial (\rho_f u_{f,i})}{\partial x_i} = 0$$
$$\frac{\partial (\rho_f u_{f,i})}{\partial t} + \frac{\partial (\rho_f u_{f,i} u_{f,j})}{\partial x_j} = -\frac{\partial p}{\partial x_i} + \frac{\partial \tau_{ij}}{\partial x_j} + f_{c,i}$$

↔

Particle Equations

Point Particles Model

$$\frac{\partial \rho_f}{\partial t} + \frac{\partial (\rho_f u_{f,i})}{\partial x_i} = 0$$
$$\frac{\partial (\rho_f u_{f,i})}{\partial t} + \frac{\partial (\rho_f u_{f,i} u_{f,j})}{\partial x_j} =$$
$$-\frac{\partial p}{\partial x_i} + \frac{\partial \tau_{ij}}{\partial x_j} + f_{c,i}$$

↔

Maxey–Riley Equation

Point Particles Model

Maxey–Riley Equation

$$m_p \frac{\mathbf{d}u_{p,i}}{\mathbf{d}t_p} = \underbrace{\frac{m_p}{\tau_p} (u_{f,i} - u_{p,i})}_{I} + \underbrace{m_f \frac{\mathrm{D}u_{f,i}}{\mathrm{D}t}}_{II} + \underbrace{\frac{1}{2} m_f \frac{\mathrm{D}u_{f,i}}{\mathrm{D}t}}_{III} - \underbrace{\frac{\mathbf{d}u_{p,i}}{\mathbf{d}t_p}}_{IV} \\ + \underbrace{6d_p^2 \sqrt{\pi \rho_f \mu_f} \int_{t_{p0}}^{t_p} \frac{\mathbf{d}}{\mathbf{d}\tau} (u_{f,i} - u_{p,i}) \frac{1}{\sqrt{t_p - \tau}} \mathbf{d}\tau}_{IV} \\ + \underbrace{(m_p - m_f) g_i}_{V} + \underbrace{\frac{1}{2} \pi \rho_f d_p^2 C_L L_i V_{rel}^2}_{VI}$$

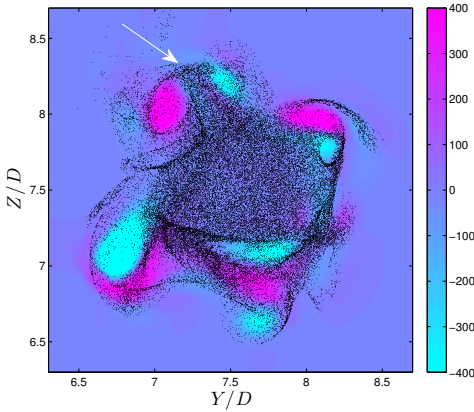
Point Particles Model

$$\frac{\partial \rho_f}{\partial t} + \frac{\partial (\rho_f u_{f,i})}{\partial x_i} = 0$$
$$\frac{\partial (\rho_f u_{f,i})}{\partial t} + \frac{\partial (\rho_f u_{f,i} u_{f,j})}{\partial x_j} =$$
$$-\frac{\partial p}{\partial x_i} + \frac{\partial \tau_{ij}}{\partial x_j} + f_{c,i}$$

↔

$$\frac{dx_{p,i}}{dt} = u_{p,i}$$
$$\frac{dv}{dt} = \frac{1}{\tau_p} (u - v)$$

Clustering in Jet Cross-Section

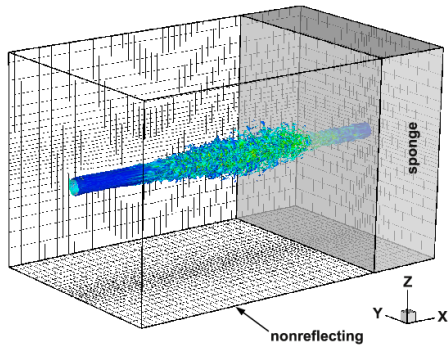


$Re_D = 1000$, $S_t = 0.2 - 0.8$, $Ma = 1.5$, Number of Particles: 10^6 ,
 $x/D = 8.3$, coloured by ω_x

Details of the Numerical Simulation

- compressible Navier–Stokes equations
- 6. order in space (compact)
- 4. order Runge-Kutta in time
- Reynolds number $Re_D = 1000 - 5000$
- Fully expanded Mach number $M_j = 1.48$

- physical domain:
 $25D \times 15D \times 15D$
- Grid resolution:
 $1024 \times 512 \times 512$



General description of Eruption Behaviour

schlieren images



General description of Eruption Behaviour

schlieren images



General description of Eruption Behaviour

schlieren images



General description of Eruption Behaviour

schlieren images



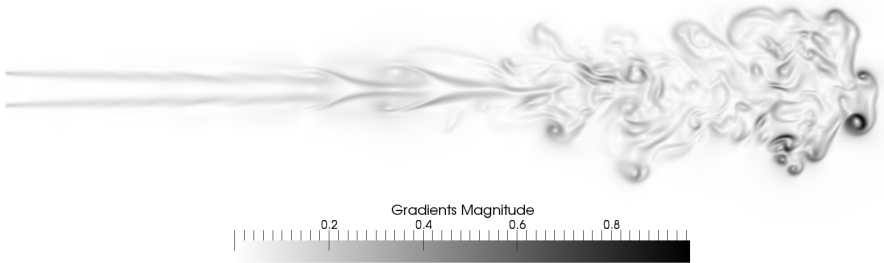
General description of Eruption Behaviour

schlieren images



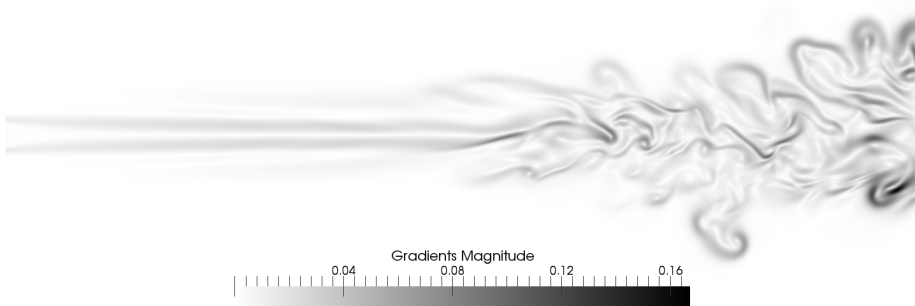
General description of Eruption Behaviour

schlieren images



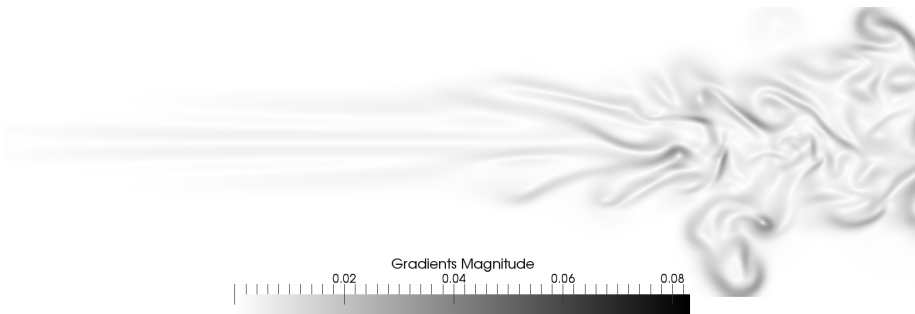
General description of Eruption Behaviour

schlieren images



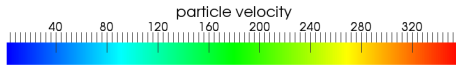
General description of Eruption Behaviour

schlieren images



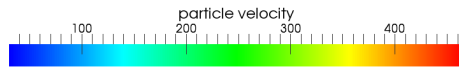
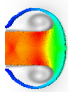
General description of Eruption Behaviour

particles coloured by velocity/schlieren - cross section



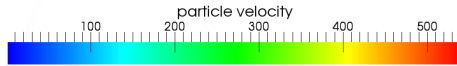
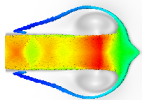
General description of Eruption Behaviour

particles coloured by velocity/schlieren - cross section



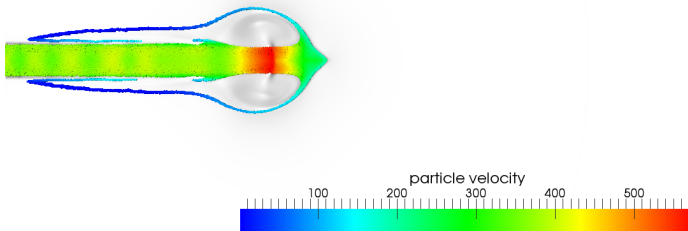
General description of Eruption Behaviour

particles coloured by velocity/schlieren - cross section



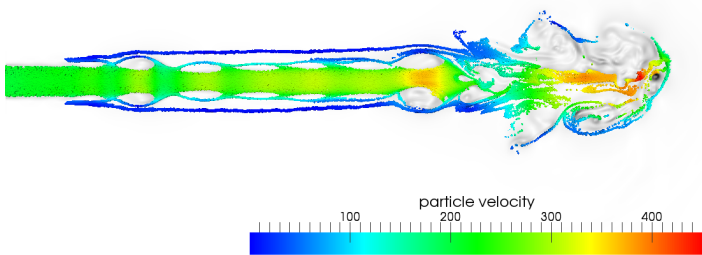
General description of Eruption Behaviour

particles coloured by velocity/schlieren - cross section



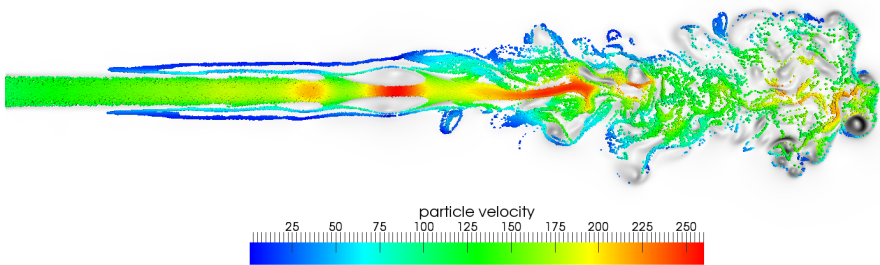
General description of Eruption Behaviour

particles coloured by velocity/schlieren - cross section



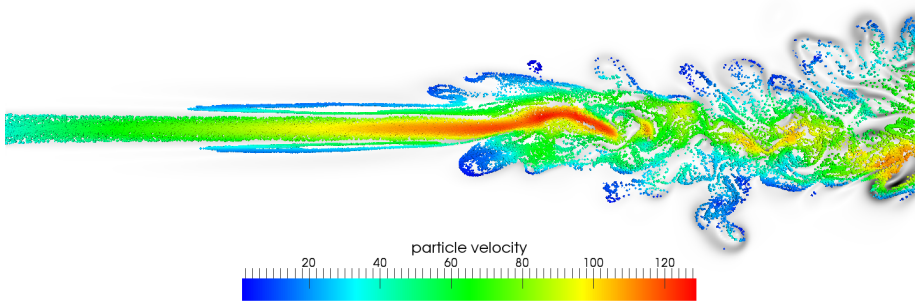
General description of Eruption Behaviour

particles coloured by velocity/schlieren - cross section



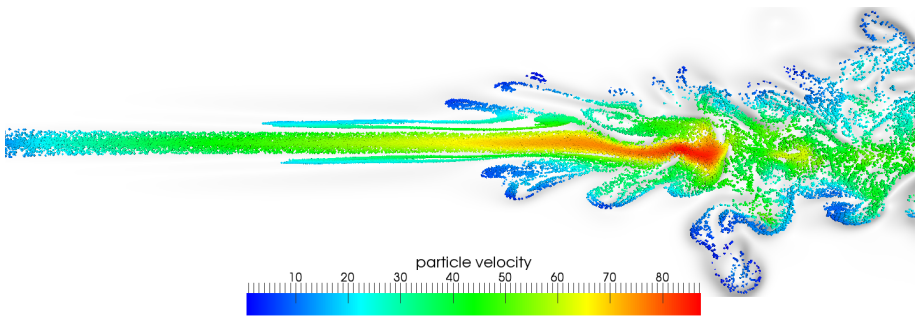
General description of Eruption Behaviour

particles coloured by velocity/schlieren - cross section



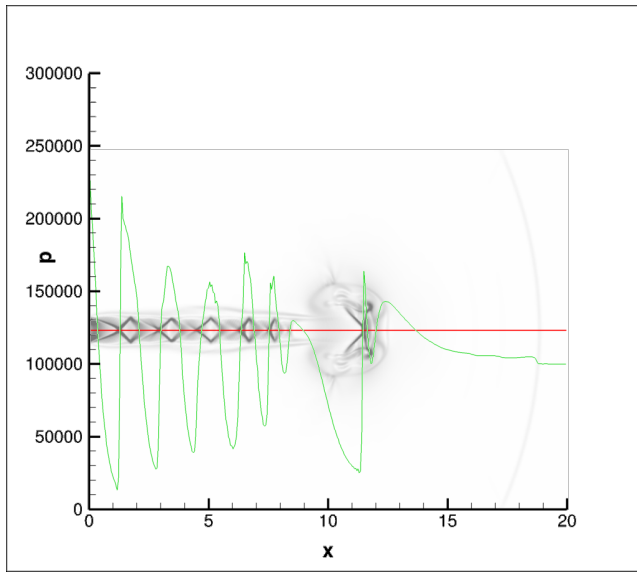
General description of Eruption Behaviour

particles coloured by velocity/schlieren - cross section



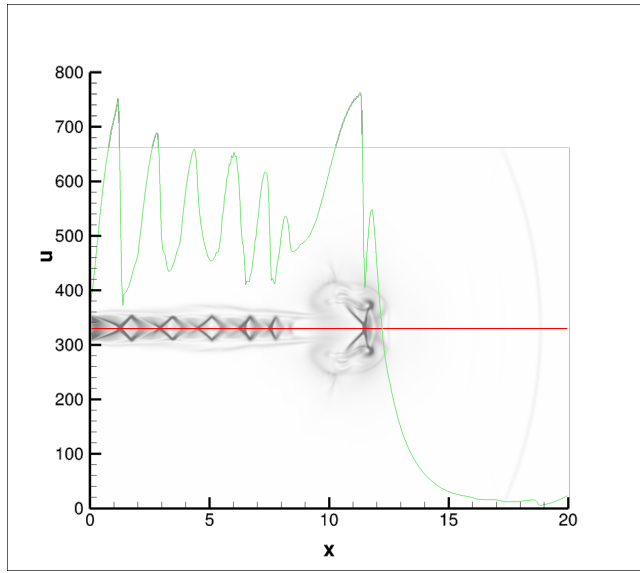
General description of Eruption Behaviour

schlieren/pressure



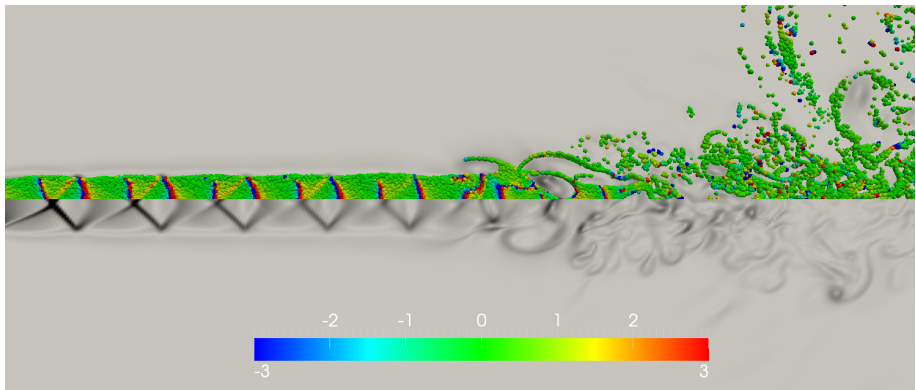
Particle Shock Interaction

schlieren/velocity



Particle Shock Interaction

schlieren



Jet noise modification due to Particles

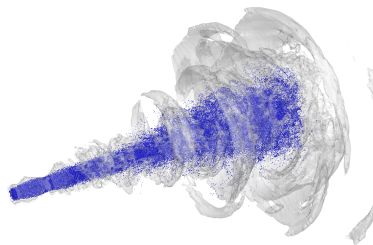


Figure: Vortical Modes, without and with particles

Jet noise modification due to Particles

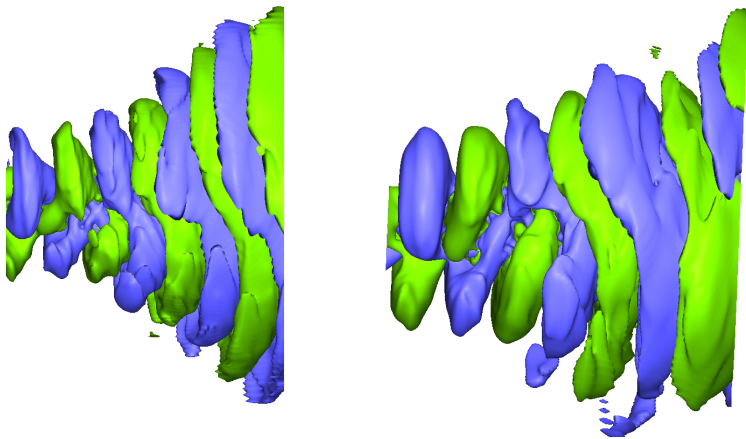


Figure: Vortical Modes, without and with particles

Jet noise modification due to Particles

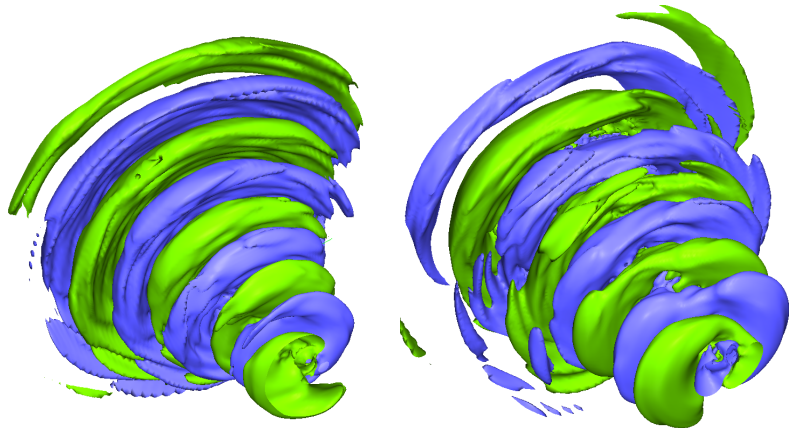


Figure: Vortical Modes, without and with particles

Jet noise modification due to Particles

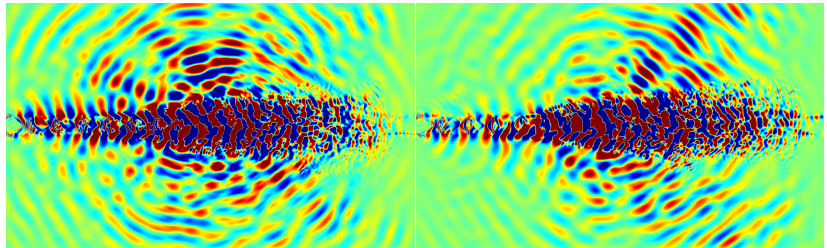


Figure: Vortical Modes, without and with particles

Jet noise modification due to Particles

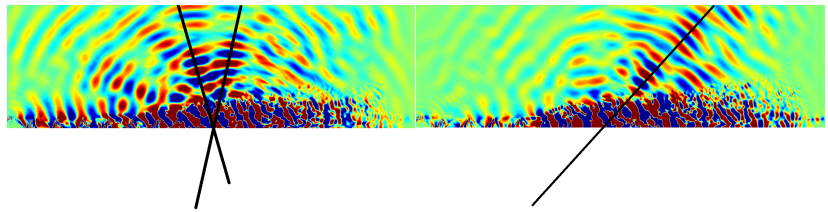


Figure: Vortical Modes, without and with particles

Jet noise modification due to Particles

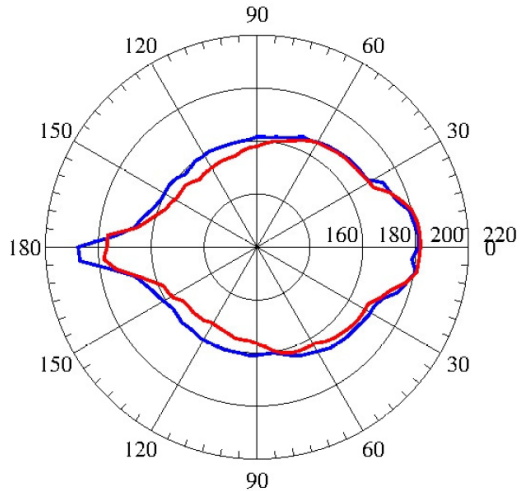


Figure: Vortical Modes, without and with particles

Particle Clustering

Jet evolution

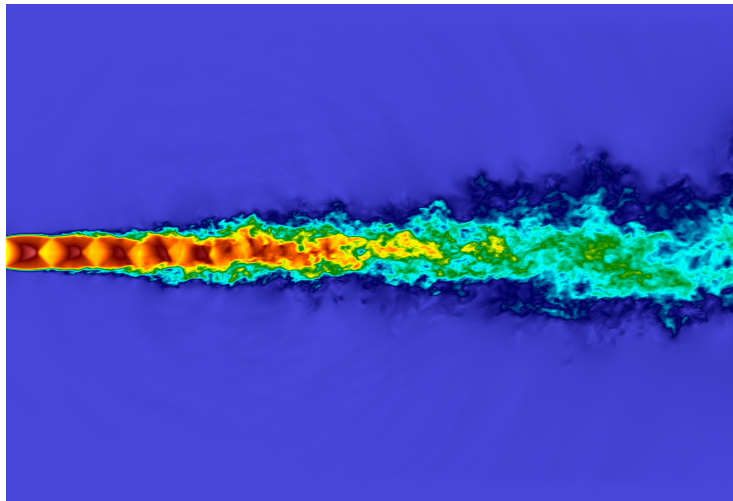
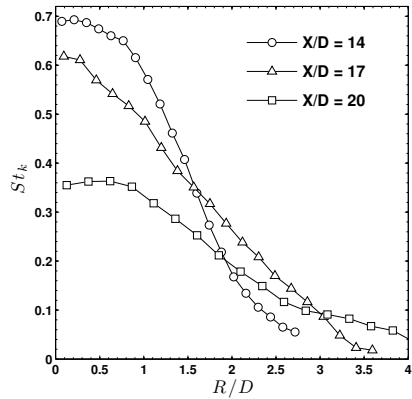
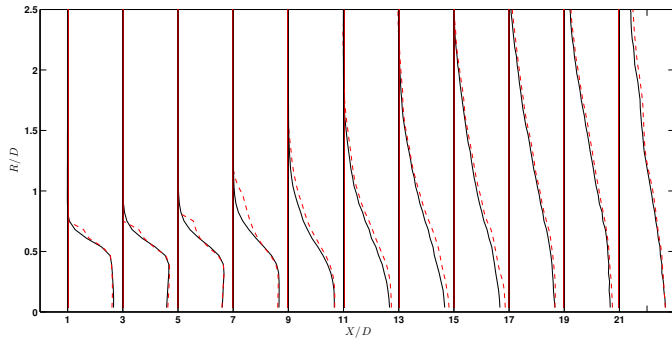


Figure: evolution of the jet shown with streamwise velocity

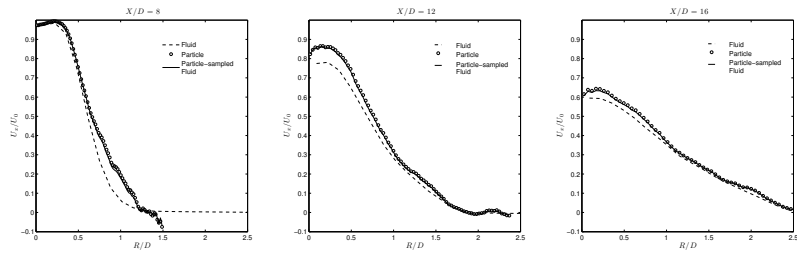
Local Stokes Number



Streamwise development of mean axial particle Velocity

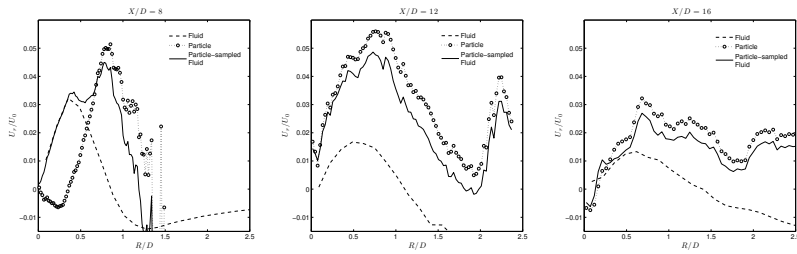


Streamwise development of mean axial particle Velocity conditional sampling of fluid velocity

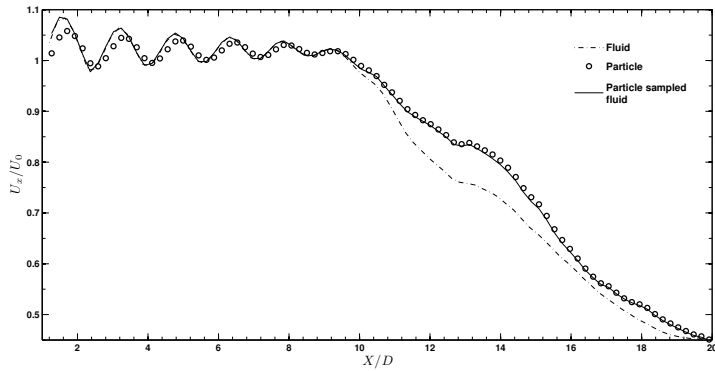


Streamwise development of mean radial particle Velocity

conditional sampling of fluid velocity



Particle Relaxation in Shock Regions



$$\frac{du_p}{dx} = \frac{1}{l_p}(u_f - u_p)$$

$$l_p = 0.29D = 290d_p$$

Particle Preferential Concentration

Invariants of the velocity gradient tensor

velocity gradient tensor

$$\frac{\partial u_i}{\partial x_j}$$

characteristic polynomial

$$p(\lambda) = \lambda^3 + P\lambda^2 + Q\lambda + R$$

Particle Preferential Concentration

conditional sampling with Q

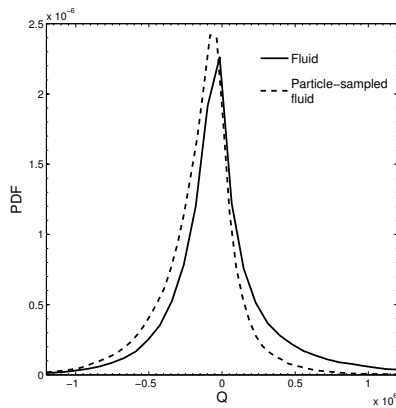


Figure: Particles prefer shear regions $Q < 0$

Particle Preferential Concentration

conditional sampling with P

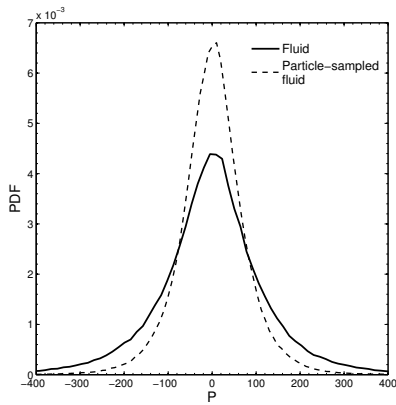


Figure: Particles prefer incompressible regions (small P)

FSLE Analysis

(Finite-Size Lyapunov Exponents as in Duncan et al. (2005) ... redefined for finite volumes vs. particle pairs)

for a control volume around x_m with radius δ_o compute

$$\delta_m = \frac{2}{N(N-1)} \sum_{i=1, i \neq j}^N \delta_{ij}$$

and define forward and reverse time constants

$$T_\rho^\pm = \min \{ T \geq 0 : \delta_m(t_o \pm T) = \rho \delta_m(t_o) \}$$

with that define

$$\lambda^\pm(\delta_o, \rho, t_o) = \frac{1}{T_\rho^\pm} \ln \frac{\rho \delta}{\delta}$$

Dependence of λ^- on δ_o

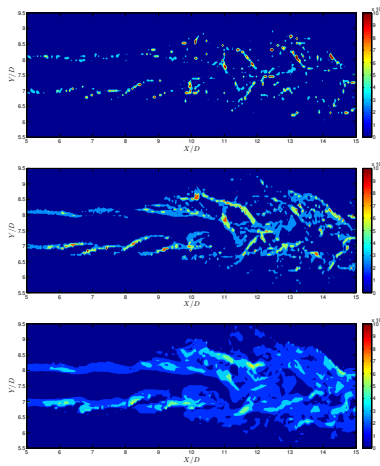


Figure: $\delta_o = \{40, 80, 240\} d_p$

Anisotropy of λ^-

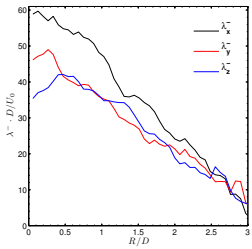
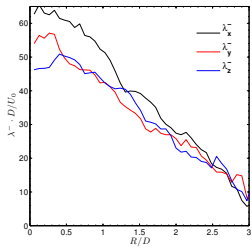
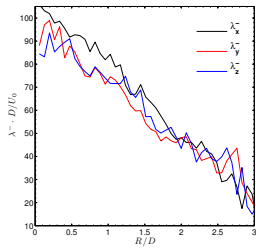


Figure: $\delta_o = \{20, 80, 120\} d_p$

Particle Preferential Clustering

conditional sampling with Q

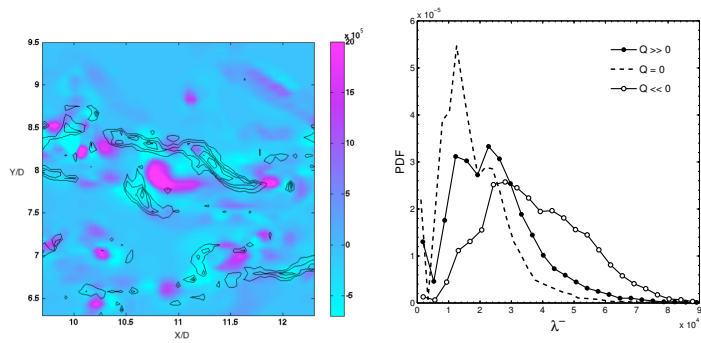


Figure: Particles converge in shear regions $Q < 0$

Particle Preferential Clustering

conditional sampling with P

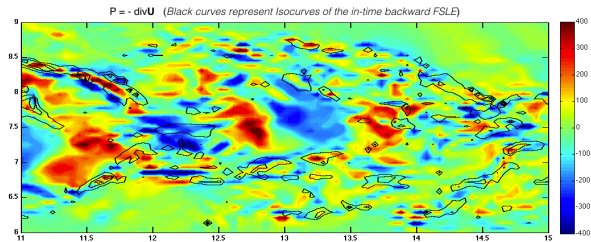


Figure: Particles somehow converge in high dilatation regions

Radial variation of the backward Lyapunov exponent

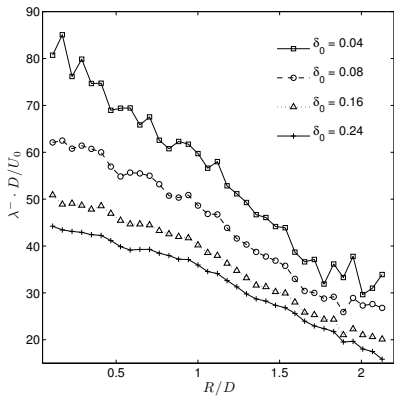


Figure: $\rho = \sqrt{2}$, average for all t_o

Radial variation of the backward Lyapunov exponent

Scaling with τ_k

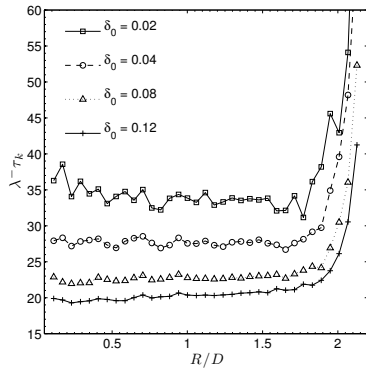


Figure: normalisation by $\tau_k = \left(\frac{\nu}{\epsilon}\right)^{\frac{1}{2}}$

Radial variation of the backward and forward Lyapunov exponent

Scaling with τ_k

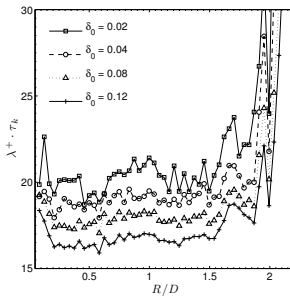
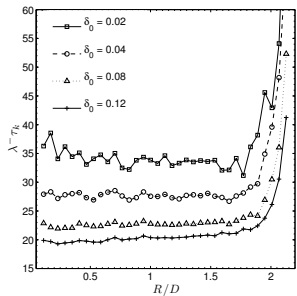
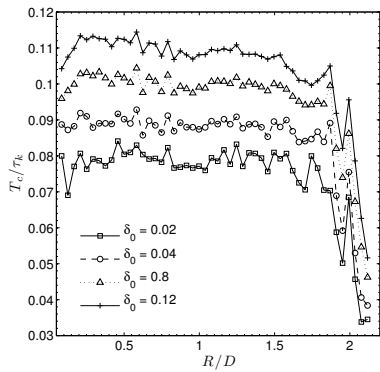


Figure: normalisation by $\tau_k = (\frac{\nu}{\epsilon})^{\frac{1}{2}}$

Cluster Forming

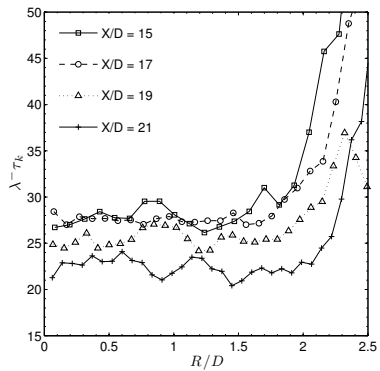
Cluster = gathering faster than dispersing

$$T_c = \frac{1}{\lambda^-} + \frac{1}{\lambda^+}$$



Streamwise variation of the backward Lyapunov exponent

Scaling with τ_k



Impinging Jet

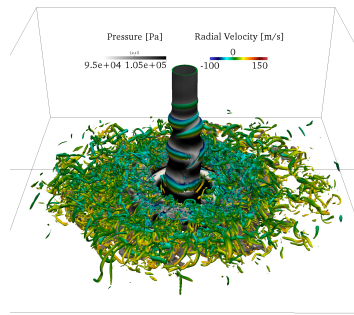


Figure: Pressure contours at the wall (movie)

Boundary Layer with particles

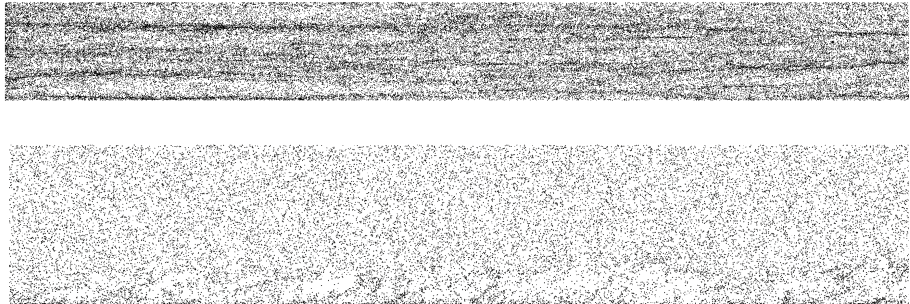


Figure: particle laden flow, compressible boundary layer, $Re_{\delta 99,e} = 5000$, $Ma = 0.8$, $512 \times 256 \times 128$, top: viscous sublayer in xz-plane; bottom: xy-plane

Boundary Layer with particles

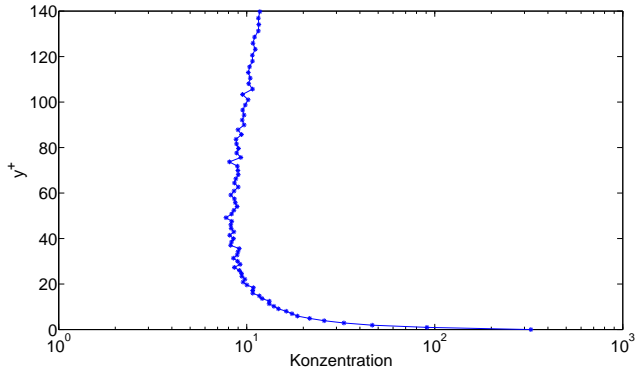


Figure: particle laden flow, compressible boundary layer, $Re_{\delta 99,e} = 5000$, $Ma = 0.8$, $512 \times 256 \times 128$, xy-plane average number density distribution as a function of the wall normal direction

Boundary Layer with particles

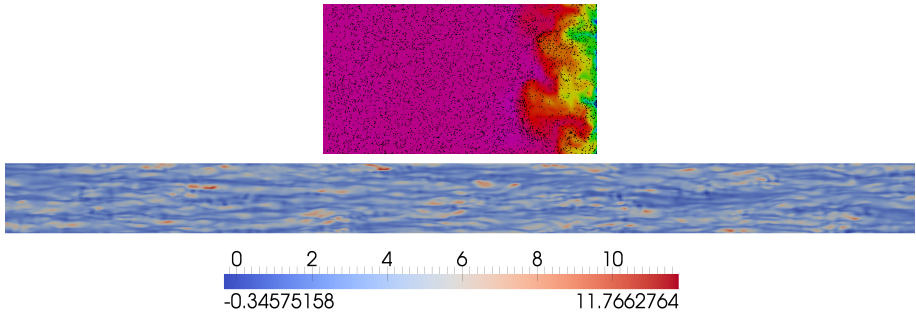


Figure: particle laden flow, compressible boundary layer, $Re_{\delta 99,e} = 5000$, $Ma = 0.8$, $512 \times 256 \times 128$, xy-plane average number density distribution as a function of the wall normal direction

Boundary Layer with particles

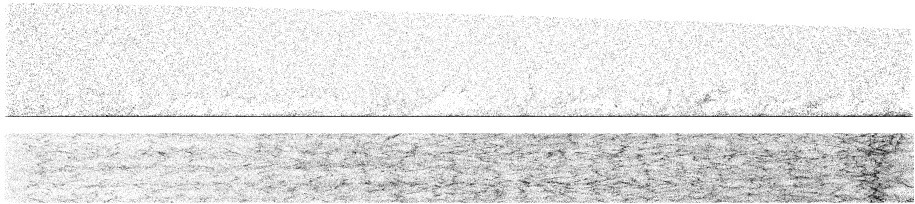


Figure: particle laden flow, compressible boundary layer, angle of attack = 22° , $Re_{\delta 99,e} = 5000$, $Ma = 0.8$, $512 \times 256 \times 128$, top: viscous sublayer in xz-plane; bottom: xy-plane

Boundary Layer with particles

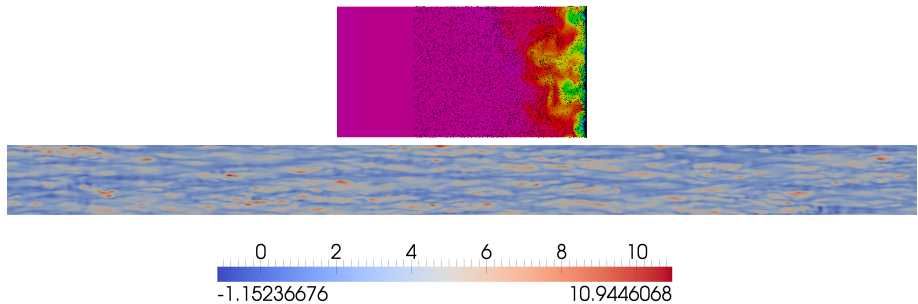


Figure: particle laden flow, compressible boundary layer, angle of attack = 22° , $Re_{\delta 99,e} = 5000$, $Ma = 0.8$, $512 \times 256 \times 128$, xy-plane average number density distribution as a function of the wall normal direction

Take home messages

- Structures are responsible for Jet noise
- Particles modify structures and sound thus sound characteristics
- Particles cluster at negative Q and small P
- Cluster forming is anisotropic
- Collecting particles at negative Q due to large λ^-
- $\lambda^-, \lambda^+, T_c$ scales with τ_k

Thanks

- Flavia Cavalcanti (Jet Computations)
- Juan Pena (Aeroacoustics)
- Antonio di Giovanni (Clustering)